Electronic Materials Letters
https://doi.org/10.1007/s13391-023-00466-9

ORIGINAL ARTICLE - ELECTRONICS, MAGNETICS AND PHOTONICS

Inkjet-Printed Flexible Ultrasensitive Chemiresistive Sensors for Aggregation Pheromone of Flour Beetles

Yunnan Fang[1] · **Manos M. Tentzeris**[1]

Received: 2 August 2023 / Accepted: 9 October 2023

Abstract

This work reports the first demonstration that a chemoresistive sensor can be used to detect the aggregation pheromone of flour beetles. To prepare the sensing element of such a sensor, a novel functionalization method was developed to amplify amine groups on the surface of carbon nanotubes (CNTs). Unlike traditional amine-amplification approaches in which amplification efficiency is significantly reduced by self-crosslinking, the current amine amplification process was self-crosslinking-free due to the use of a home-made compound in which amine groups were protected by Boc (tert-butyloxycarbonyl) protecting groups and could be deprotected as needed. The inkjet ink formulated from the functionalized CNTs, together with an amine-rich compound and a commercial silver nanoparticle-based inkjet ink, was used to fabricate (via inkjet-printing and drop-casting) lightweight, flexible, and miniature-sized chemiresistive sensors for 4,8-dimethyldecanal (DMD), a compound known to be the aggregation pheromone of several species of flour beetles. A home-built gas sensing system, including a commercial gas generator, a DMD permeation tube with its emission rate certified, a data-acquisition system, and some home-developed LabVIEW-based programs, was utilized to perform the DMD sensing trials. The sensors showed ultra-high sensitivity to synthetic aggregation pheromone DMD, as indicated by their prompt and significant responses to 100 ppb DMD vapor. A mechanism for the sensitive sensing of DMD is proposed.

Graphical Abstract

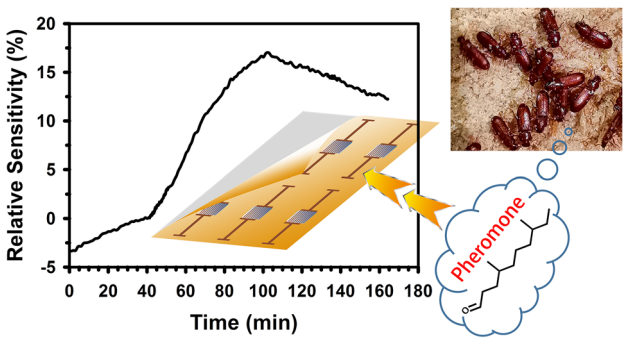

Keywords Chemiresistive gas sensors · Inkjet printing · 4,8-Dimethyldecanal · Aggregation pheromone · Flour beetles · Carbon nanotubes

✉ Yunnan Fang
yunnan.fang@mse.gatech.edu

[1] School of Electrical and Computer Engineering, Georgia Institute of Technology, Atlanta, GA 30332, USA

Published online: 08 November 2023

1 Introduction

According to Karlson and Lüscher who first defined the portmanteau word "pheromone", pheromones are "substances which are secreted to the outside by an individual and received by a second individual of the same species, in which they release a specific reaction, for example, a definite behavior or a developmental process" [1]. Pheromones have been found in plants [2] and almost every part of the animal kingdom [3].

Pheromones can be used for a number of applications. For example, they can be used as repellents to drive pest insects away from a particular area [4], as attractants to lure pest insects to a designated place for elimination [5–7], or as modulators to regulate the foraging behavior of insects [8]. For example, sex pheromones have been used for mating disruption, detection, population monitoring, mass trapping and annihilation [9], and for sensory stimulation to collect increased amount and quality of semen for the purposes of artificial insemination [10, 11]; synthetic aggregation pheromones have been used to attract insects [12]; trail pheromones have been used to disrupt the trails insects followed to the food sources [13–15].

Pheromones have been sensed with various ways. Traditionally, pheromones are sensed with bulky equipment-based methods such as ion mobility spectrometry (IMS), gas chromatography-mass spectrometry (GC–MS), and nuclear magnetic resonance (NMR). Even though exhibiting excellent sensitivity and selectivity, this type of methods is usually associated with bulky equipment, lengthy sample preparation, and solvent management. Another major type of sensors for pheromones is biosensors, in which there is a biological recognition component. The biological recognition component can be a living animal (such as a bee [16] or dog [17]), an isolated animal organ (such as an insect head [18] or antenna [19, 20]), or a protein [21–23]. However, living animal-based biosensors not only suffer from fatigue after some time and become less sensitive but also need long-time training. Other biological components either have to work in a solution or readily dry out under their working conditions. Other types of pheromone sensors that have been scarcely reported include metal oxide-based chemiresistive sensors [24] and MEMS-based optical sensors [25].

One of the pheromones flour beetles emit is aggregation pheromone. A compound, 4,8-dimethyldecanal (DMD), has been well known to be the aggregation pheromone of the confused flour beetles (*Tribolium confusum*), red flour beetles (*Tribolium castaneum*), and *Tribolium freeman* flour beetles [26]. This aggregation pheromone attracts both males and females [27]. It has been reported that 1 male adult of red flour beetle can averagely produce 1.265 mg of DMD in 2 days [28].

Flour beetles are serious pests of stored agriculture products. They exist worldwide and are commonly found in a variety of places such as processing plants, mills, retail stores, and granaries. In addition to eating almost all the grain-based products such as cereal products, coffee, pulses, nuts, and spices, they also contaminate the products with dead bodies, feces, and secretions. The damage caused by flour beetles is causing significant economic loss.

Apparently, detection of the aggregation pheromone DMD is an efficient way to monitor the population of the aforementioned 3 types of flour beetles. To the best of our knowledge, DMD detection with a chemiresistive sensor has never been reported.

This work reports the first demonstration that a chemoresistive sensor can be used to detect the aggregation pheromone of flour beetles with ultra-high sensitivity.

2 Experimental Details

2.1 Functionalization of Carbon Nanotubes

A step-by-step schematic showing the functionalization of carbon nanotubes is shown in Fig. 1. Briefly, a small sheet (for example 10 mm × 10 mm) of semiconducting single wall carbon nanotube (SWCNT) film (IsoNanotubes-S. NanoIntegris Technologies, Inc., Boisbriand, Quebec, Canada) was immersed in dimethylformamide (DMF) and then sonicated slightly (10 s at power level 10) with a probe sonicator (Sonicator 3000, Misonix, Farmingdale, NY, USA). After a short centrifugation (4, 500×*g*, 2 min), the resulting SWCNT particle suspension was incubated with a mixture solution of concentrated sulfuric acid and concentrated nitric acid (H_2SO_4:HNO_3 = 3:1) and sonicated in a bath ultrasonic cleaner for 3 h at 40 °C (Fig. 1 step a), followed by washing 3 times with DI water with centrifugation (4, 500×*g*, 2 min) between rinses and after the last rinse. This process introduced carboxyl groups to the SWCNT surface. The carboxyl group-terminated SWCNT particles were incubated for 1 h with a 5.15 mM EDC/11.05 mM Sulfo-NHS solution in a 100 mM MES buffer containing 0.15 M NaCl (pH 5.85) (Fig. 1 steps b and c). The SWCNT particles were then washed first with DI water and then with a PBS buffer (100 mM NaH_2PO_4, 100 mM Na_2HPO_4, and 150 mM NaCl, pH 7.2) with a short centrifugation (4, 500×*g*, 2 min) between rinses and after the last rinse. The SWCNT pellets were collected and incubated with a 10 wt% tris (2-aminoethyl) amine (TAEA) solution in DMF for 1 h to introduce surface amine groups to the SWCNTs (Fig. 1 step d). After washing 3 times with DMF, the resulting amine-terminated structure was then incubated for 30 min at room temperature on a rocker with a dimethyl sulfoxide-based 1 mg/ml

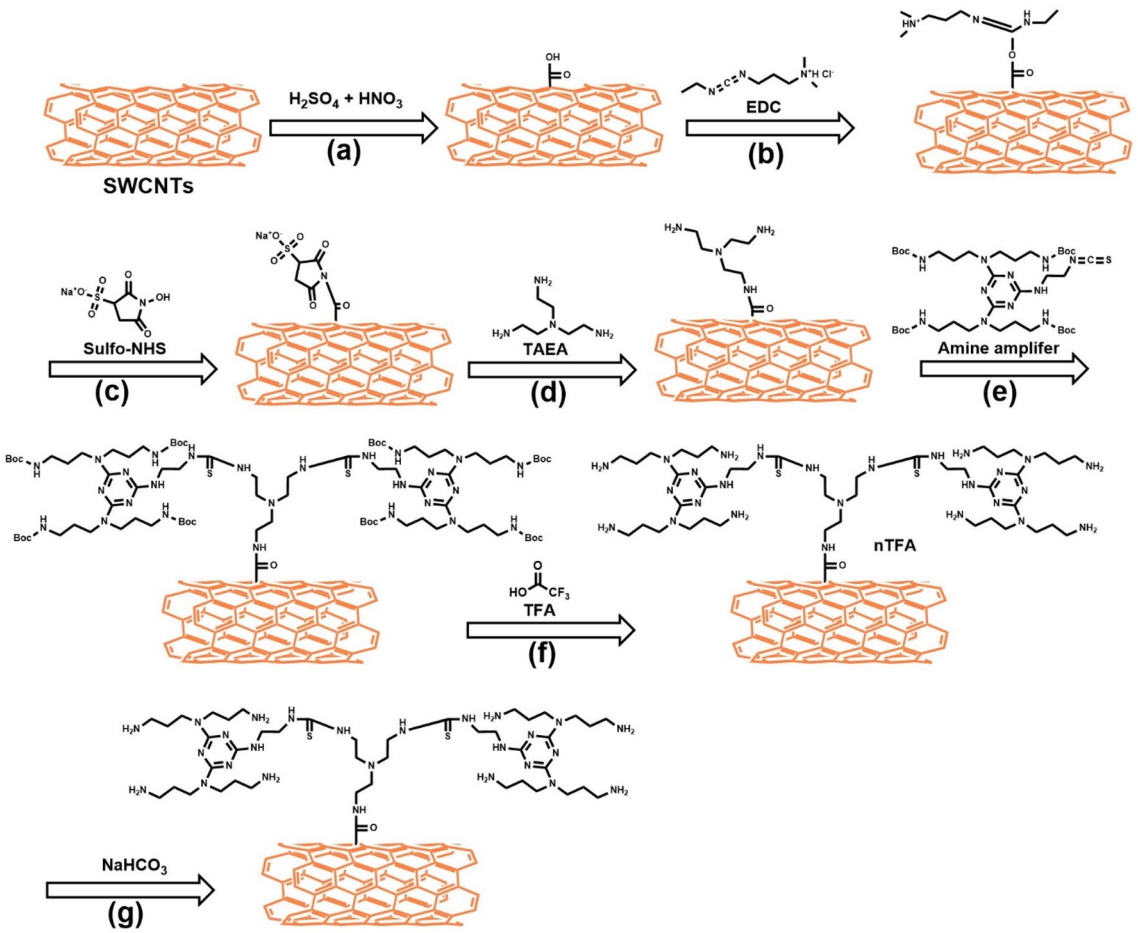

Fig. 1 Schematic for functionalization of semiconducting carbon nanotubes

solution of a home-synthesized compound (Amine amplifier. A gift from Dr. Junxiang Zhang of Georgia Institute of Technology) containing an isothiocynate group and 3 tert-butyloxycarbonyl- (Boc-) protected amine groups (Fig. 1 step e), followed by rinsing 3 times with isopropanol with a short centrifugation (4, 500×*g*, 2 min) between rinses and after the last rinse. The SWCNT pellets were then suspended in a dichloromethane-based solution of 5 v/v % trifluoroacetic acid and incubated on a rocker for 20 min at room temperature to deprotect the Boc groups on the SWCNT surface (Fig. 1 step f), followed by rinsing 3 times with isopropanol with a short centrifugation (4, 500×*g*, 2 min) between rinses and after the last rinse. The SWCNT pellets were then suspended in an aqueous solution of 1 M sodium bicarbonate containing 50% isopropanol and incubated on a rocker for 20 min at room temperature (Fig. 1 step g). This step neutralized the trifluoroacetic acid that remined in the SWCNT suspension. After rinsing 3 times with DI water and 1 time with isopropanol with a short centrifugation (4, 500×*g*, 2 min) between rinses and after the last rinse, the SWCNT pellets were suspended in an appropriate amount of DMF and sonicated with the sonicator until a homogeneous suspension was obtained.

2.2 Fabrication of Gas Sensors

The sensor fabrication process is summarized in Fig. 2a. Generally, the process included inkjet-printing of sliver-based interdigitated electrodes (IDEs), inkjet-printing of functionalized carbon nanotubes (CNTs), and drop-casting of TAEA, as detailed below.

2.2.1 Inkjet-Printing of Interdigitated Electrodes

Figure 2b shows the schematic illustration of an IDE used in this work. It consisted of 2 finger-lead structures. The fingers are separated by small gaps. The finger width and the finger spacing are 70 µm and 346 µm, respectively. The IDEs were inkjet printed on a polyimide film (Kapton® HN 500, DuPont, Wilmington, DE, USA) with a drop-on-demand piezoelectric inkjet printer (DMP-2831, Fujifilm Dimatix, Inc., Santa Clara, CA, USA) and a silver nanoparticle-based

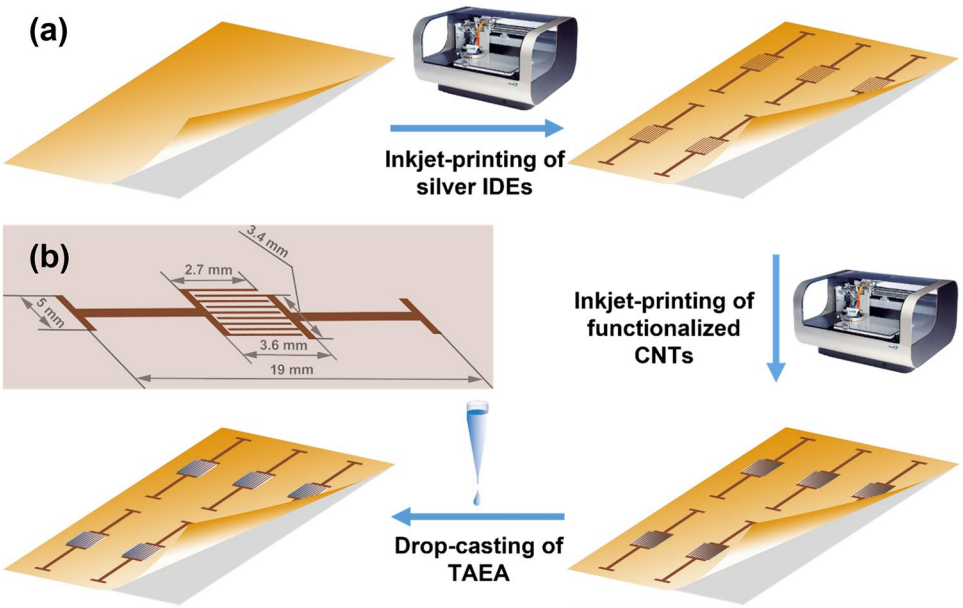

Fig. 2 **a** Schematic for functionalization of semiconducting carbon nanotubes. **b** Schematic illustration of an interdigitated electrode used in this work. The line width and spacing of the electrode fingers, which are not shown in the illustration (for tidiness purposes), are 70 µm and 346 µm, respectively

ink (EMD5730, Sun Chemical Corporation, Parsippany, NJ, USA). The silver nanoparticle-based ink was printed (3 passes) on the polyimide film followed by sintering at 150 °C for 30 min. A platen temperature of 45 °C, a 10-picoliter cartridge, and a drop spacing of 20 µm were used during the inkjet-printing process.

2.2.2 Inkjet-Printing of Functionalized CNTs

The 2 finger-lead structures of an IDE were physically separated (as illustrated in Fig. 2b). In order for an IDE to function as a chemiresistive sensor, the gaps between its fingers had to be bridged with a conducting or semi-conducting material, so that its 2 finger-lead structures were electrically conductively connected. In this work, the functionalized semi-conducting CNTs were inkjet-printed (4 layers, with the same inkjet-printer as the one for the IDEs) on top of the finger area (i.e., the central region) of an inkjet-printed silver IDE to bridge the finger gaps, followed by drying at 140 °C for 10 min. A platen temperature of 60 °C, a 10-picoliter cartridge, and a drop spacing of 20 µm were used during the inkjet-printing process. A tiny drop (2.5 µl) of a 5 v/v% TAEA solution in isopropanol was dropcasted (with a pipette) onto the top of the resulting CNT patch, followed by drying at 140 °C for 10 min.

2.3 Gas Sensing

The setup for the sensing of DMD vapor is shown in Fig. 3. Figure 3a, b shows the schematic illustration and most of the actual components, respectively, of the setup. Synthetic pheromone DMD was purchased from Prof. Michael Chong at the University of Waterloo, Canada and sent to the KIN-TEK Laboratories, Inc. (La Marque, TX, USA) where a disposable permeation tube (Fig. 3c) with this compound was custom-made and its emission rate certified. The permeation tube, with a KIN-TEK serial number of 64742, was certified to have a target emission rate of 269 ng/min at 100 °C. The permeation tube was housed in a glass adapter bottle (KIN-TEK Laboratories, Inc.) in the oven of a FlexStream™ Gas Standards Generator (KIN-TEK Laboratories, Inc.). Synthetic air (Airgas, Radnor, PA, USA) was used as the carrier gas for the DMD vapor. The temperature of the oven was set to 100 °C and the concentration of the DMD vapor was determined based on Eq. (1):

$$C_{ppmv} = \frac{E \times 22.41}{MW \times F} \quad (1)$$

where C_{ppmv} = generated concentration (ppm by volume) of DMD vapor. E = emission rate (ng/min) of DMD from the permeation tube at the certification oven temperature (269 ng/min at 100 °C, as certified by KIN-TEK Laboratories, Inc.). MW = molecular weight of DMD, 184.32 g/mol. 22.41 = volume (L) of 1 mol of vapor at standard temperature and pressure (i.e., STP) conditions of 0 °C and 760 mmHg of pressure. F = flow rate (sccm) of the carrier gas (synthetic air).

By keeping the oven temperature at 100 °C and setting the flow rate of the carrier gas to 327, 65, and 33 sccm, a DMD vapor concentration of 100, 500, and 1000 ppb, respectively, was generated from the permeation tube and guided to the sensor box in which the sensors were hooked up. The sensor box was home-made with a 1.0-L Snapware® airtight food storage container. A sensing trial was performed with a data acquisition system (NI Corporation, Austin, TX, USA) automated with home-developed LabVIEW-based programs.

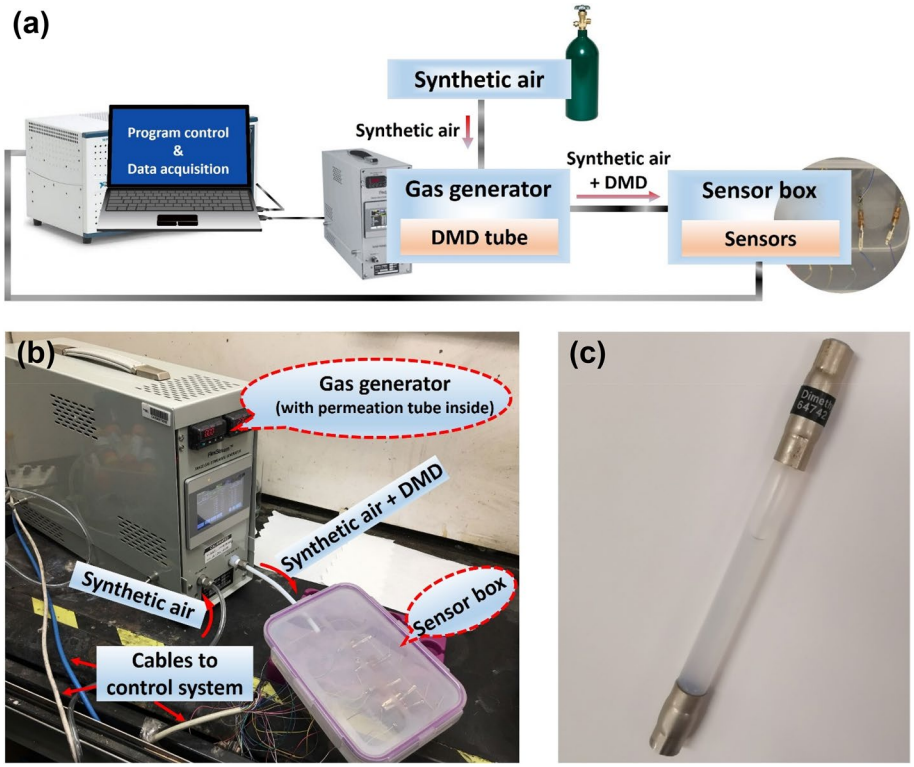

Fig. 3 Setup for the sensing of DMD vapor. **a** Schematic diagram showing all the components in the system and their connections. **b** Optical image showing some components (gas generator, sensor box, gas inlet and outlet, and the cables connecting the gas generator/sensors to the program control and data acquisition system). **c** Custom-fabricated and emission rate-certified DMD permeation tube installed inside the gas generator

The electrical resistance changes of a sensor upon exposure to either the carrier gas (synthetic air) or the DMD vapor in synthetic air were automatically recorded by the data acquisition system.

3 Results and Discussions

Based on their chemical structures, insect pheromones can fall into a wide range of chemical categories (such as phenol [29, 30], alcohol [12, 31–34], acid [30, 35], terpene [36, 37], ester [30, 34, 36], and aldehyde [12, 26, 27, 36]). DMD is chemically an aldehyde. Figure 4 shows the image of some male confused flour beetles and the chemical structure of the aggregation pheromone (DMD) they emit. This work took the advantage of the chemical reaction between an aldehyde and a primary amine on the sensor surface forming an imine derivative and eliminating water (Fig. 5). Even though selectivity testing with other vapors was not performed in this work, we speculate that our sensors are probably not able to distinguish vapors which can readily react with primary amines. Particularly, our sensors probably won't be able to distinguish aldehyde-based pheromones emitted from different species of insects, but can differentiate an aldehyde-based pheromone from most (if not all) other types of pheromones.

We have previously developed a straightforward and general method to introduce surface primary amine groups and then dendritically amplify the resulting surface amine groups in a layer-by-layer fashion [38, 39]. Specifically, a polyamine compound, TAEA, and a polyacrylate compound, dipentaerythritol penta-/hexa-acrylate (DPEPHA), were used to

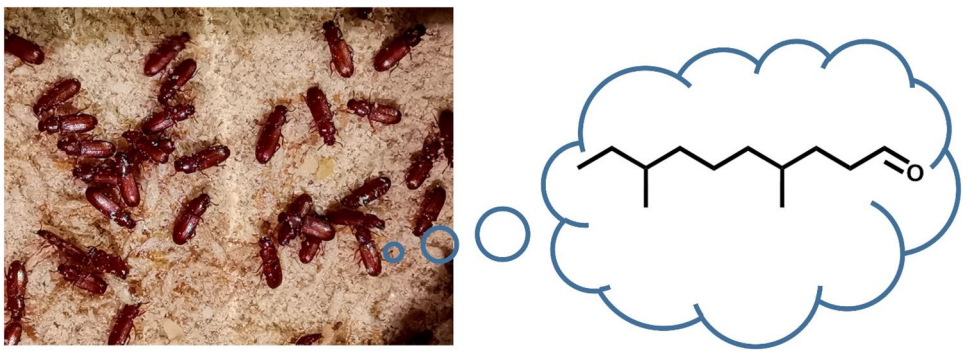

Fig. 4 Optical image of some male confused flour beetles and the chemical structure of the aggregation pheromone (DMD) they emit. The confused flour beetles were provided by Dr. Clark "Chuck" Klein from Urban Pest Control at BASF Corporation (Research Triangle Park, NC, USA)

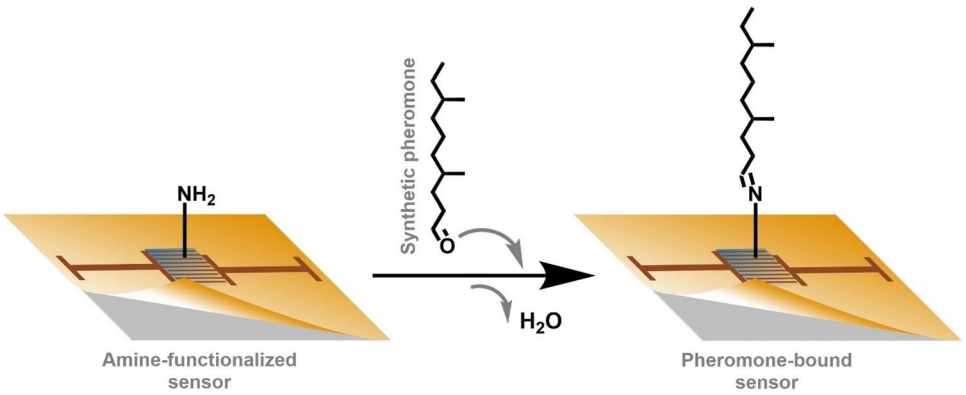

Fig. 5 Chemical reaction between a sensor and the synthetic pheromone DMD

dendritically amplify amine groups, taking advantage of the Michael addition reaction between a primary amine group and an acylate group. During the layer-by-layer amplification process, amine groups and acrylate groups were alternately grafted to the substrate surface. Surface amine groups or acylate groups were amplified with increasing layers. However, this amplification method has a drawback: self-crosslinking might happen during the amplification process. Figure 6 shows examples of this method with and without self-crosslinking. The self-crosslinking wastes the involving functional groups (e.g., the amine and acrylate groups in the examples shown in Fig. 6) which can be otherwise used for amine/acrylate amplification, and consequently, the amplification efficiency is significantly reduced. Unlike the aforementioned amine-amplification method in which 2 compounds (i.e., a polyamine and a polyacrylate) were used, the current amine-amplification method employed a single compound containing 3 Boc-protected amine groups which could be deprotected as needed. With this method, amine groups were amplified by a factor of 4 after each cycle.

Figure 7a shows an optical image of a flexible, lightweight, and miniature-sized DMD sensor fabricated on a Kapton® polyimide film. Figure 7b, which is a scanning electron microscopic image of this sensor, shows inkjet-printed CNTs dispersed on one of the IDE fingers (right side) as well as on a substrate area between 2 IDE fingers (left side). The flexibility of all the sensor components (Kapton® substrate, silver traces, and functionalized CNTs), as well as the robust, lightweight, and miniature-sized nature of the sensors enabled excellent wearability and resistance to harsh environments.

Figure 8 shows the real-time resistance changes (Fig. 8a, c, e) and relative sensitivity changes (Fig. 8b, d, f), as a function of time, of 3 sensors before and after exposure to

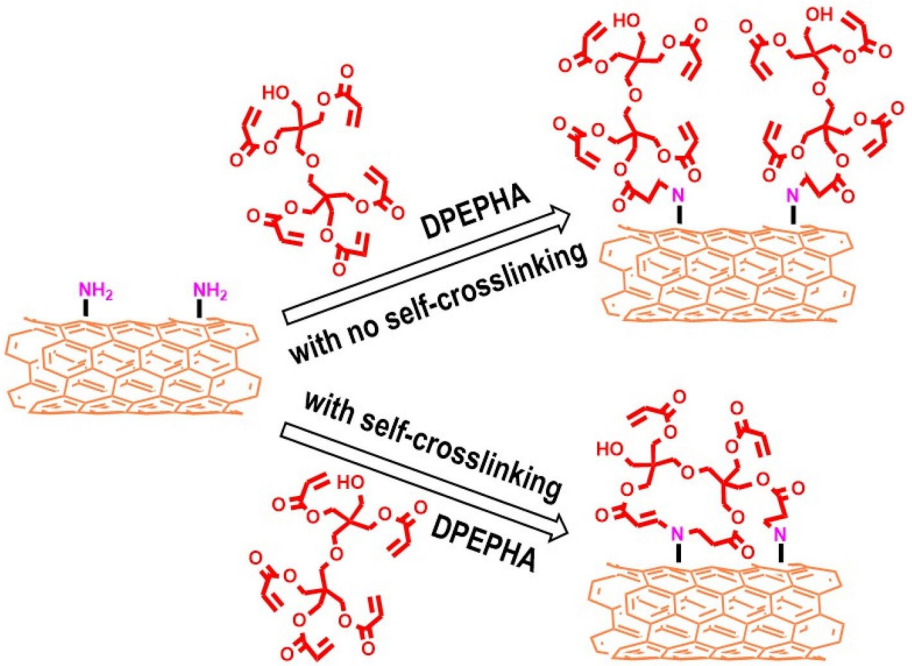

Fig. 6 Examples of Michael addition with and without self-crosslinking

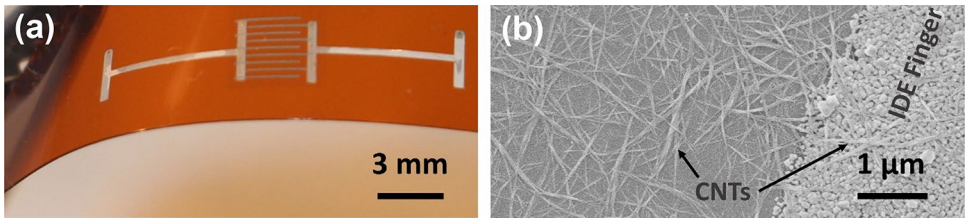

Fig. 7 Optical (**a**) and scanning electron microscopic (**b**) images of a DMD sensor fabricated on Kapton® polyimide substrate

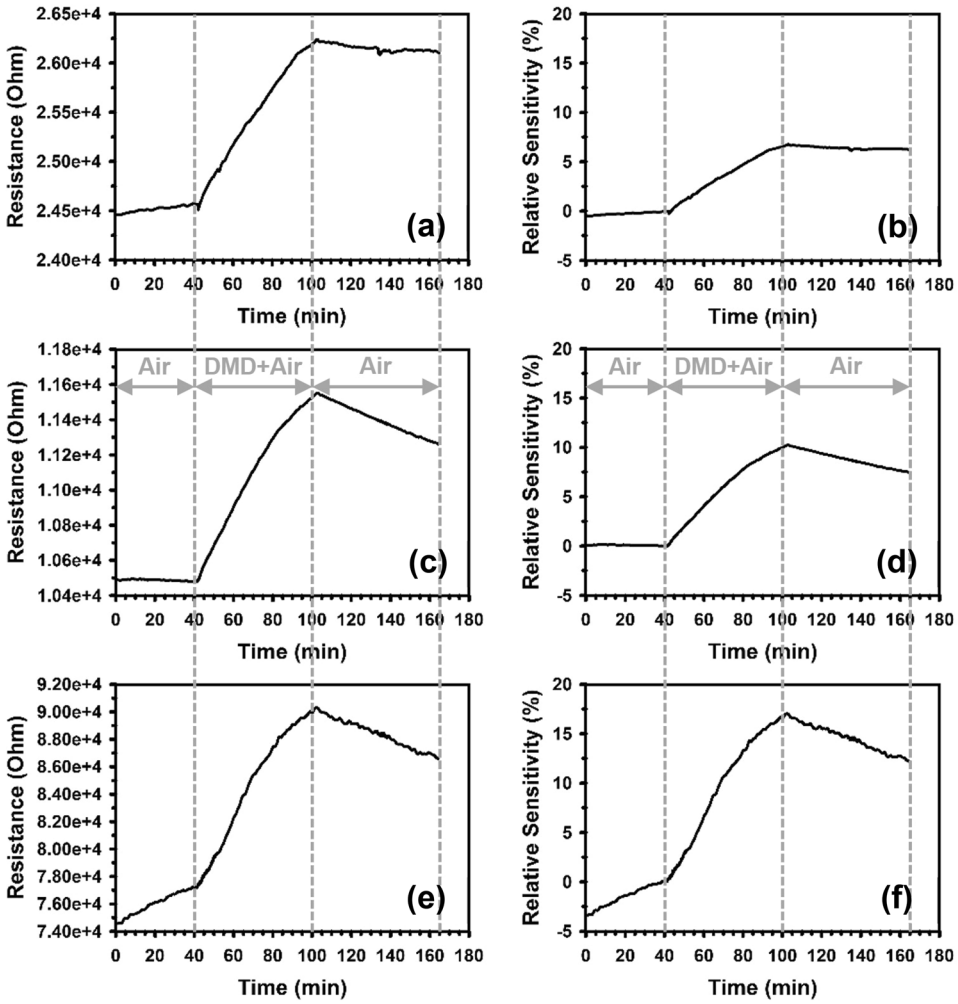

Fig. 8 Sensing profiles of 3 sensors before and after exposure to DMD vapor of 100 (**a**, **b**), 500 (**c**, **d**), and 1000 (**e**, **f**) ppb, respectively. **a**, **c**, **e** are the real time resistance profiles of the 3 sensors, while **b**, **d**, **f** are the relative sensitivity profiles corresponding to the resistance profile in **a**, **c**, **e**, respectively

DMD vapor of 100, 500, and 1000 ppb, respectively. At the early stage of the sensing process (0–40 min), in which the sensors were exposed to the carrier gas only (with no DMD vapor released), the resistance baseline of all the 3 sensors drifted to a greater or lesser extent. The reason for the baseline drift is unclear, but such drift has been common for polymer-based sensors and reported in a number of reports [40, 41]. Despite such baseline drift, the resistance jump upon exposure to DMD vapor was still apparent for all the 3 sensors. There was a small response delay for the 2 sensors that were sensing a DMD vapor concentration of 100 (Fig. 8a, b) and 500 (Fig. 8c, d) ppb, respectively (the response delay of the 100-ppb and 500-ppb sensors was ~ 2 and ~ 1 s, respectively). The 1000-ppb sensor (Fig. 8e, f) seemed to respond immediately upon the launch of the DMD vapor. We speculate that the response delays were due to the relatively large volume (1.0 L) of our home-made sensor box which was designed to test multiple (up to 8) sensors at the same time (Fig. 3b). Indeed, it took time for the DMD vapor to fill the relatively large box to reach a DMD concentration which was detectable for the sensors.

As shown in Fig. 8, the DMD vapor was released for 60 min (time range 40–100 min), during which the resistance of all the 3 sensors kept increasing. Upon stopping the DMD vapor (at the 100th min), the resistance drop of all the 3 sensors did not immediately happen. Instead, there was a

small delay for all the 3 sensors (the delay for the 100-, 500- and 1000-ppb sensors was ~3, ~3, and ~2 s, respectively), which was due to the relatively slow dissipation of the DMD vapor from the sensor box (the mixture of the synthetic air and DMD vapor was dissipated from the sensor box via the holes through which the connecting cables passed the sensor box). After exposure to their respective (100, 500 or 1000 ppb) DMD vapor for 1 h, the 3 sensors reached a relative sensitivity of 6.8% (Fig. 8b), 10.2% (Fig. 8d), and 17.0% (Fig. 8f), respectively, indicating that the sensors were ultra-sensitive to DMD. The relative sensitivity (S) is defined by Eq. (2):

$$S = \left(R - R_0\right)/R_0 \quad (2)$$

where R and R_0 are the resistance values of a sensor at a particular time after and right before, respectively, the sensor was exposed to the target vapor.

Even though the resistance baseline drift negatively affected, to some extent, our observations of sensor recovery after the DMD release had been stopped, it was still clear that the recovery of all the sensors was very slow (Fig. 8). Among the DMD molecules that bound to a sensor during a sensing trial, most of them bound to the sensor via stable covalent bonding (as shown in Fig. 5) and only a small portion bound to the sensor via some other relatively weaker interactions such as physical absorption. Under our experimental conditions (i.e., ambient conditions), the covalent bonding between the functionalized CNTs and the DMD molecules was stable, and it is difficult to release a covalently bound DMD molecule from the sensor. Consequently, under our experimental conditions a sensor that had been exposed to DMD vapor would not be able to fully recover to its initial state, and this sensor, which already had some DMD molecules bound to it, would not be as sensitive to DMD as it was when it was fresh (i.e., with no DMD molecules bound to it). For this reason, we did not use the same sensor to sequentially sense the 3 different DMD concentrations. Additionally, since in practice, multiple sensing trials have to be performed with the same sensor and varying DMD concentrations in order to determine the minimum detectable concentration (MDC) of the sensor, MDCs of the sensors were not determined in this work. More work is needed to optimize the functionalization of CNTs, minimize the baseline drift of the electric resistance, explore efficient approaches to recover used sensors, and determine the MDCs of the sensors.

Kapton® polyimide films were used in this work as the substrate on which the DMD sensors were fabricated, due to their excellent flexibility, mechanical properties, and chemical and thermal stability. It is worth mentioning that the sensors can also be fabricated with good adhesion on a wide range of flexible or rigid substrates, such as synthetic paper, polyethylene terephthalate (PET) films, Rogers® dielectric laminates, ceramic (such as ZrO_2, Al_2O_3) sheets, FR4 laminates, and silicon wafer. Sometimes surface modification to a substrate is necessary to ensure good adhesion between the substrate and the sensors fabricated on it, as shown in some of our previous work [42–44]

Encouraged by the great sensitivity of the DMD sensors described in this work, we have successfully detected the aggregation pheromone of live flour beetles with similarly fabricated sensors. The efforts with live flour beetles will be described in a separate report.

4 Conclusions

A novel amine-amplification approach, with the use of a home-synthesized and protecting group-containing compound, was developed to introduce dense amine groups to the CNT surface. This approach differs from traditional amine-amplification approaches in that no self-cross-linking was involved. Flexible, lightweight, and miniature-sized chemiresistive sensors were fabricated, for the first time, for the detection of DMD, the aggregation pheromone of the *Tribolium confusum, Tribolium castaneum*, and *Tribolium freeman* flour beetles. DMD vapor of different concentrations was sensed with such fabricated sensors. These sensors were ultra-sensitive to DMD, as indicated by their prompt and significant response to 100 ppb DMD vapor. The sensing mechanism is thought to be the chemical reaction between the aldehyde group of DMD and the primary amines on the sensor surface.

Acknowledgements This work was supported by the BASF Corporation via a project entitled "Smart Agriculture and Smart Farming Applications" (Award No.: AWD-103013. Program manager: Dr. Clark "Chuck" Klein). We thank Andrew David Fang for proof-reading the manuscript.

Declarations

Conflict of interest The authors declare no conflict of interest.

References

1. Karlson, P., Luscher, M.: Pheromones—new term for a class of biologically active substances. Nature **183**(4653), 55–56 (1959). https://doi.org/10.1038/183055a0
2. Sekimoto, H.: Plant sex pheromones. In: Litwack, G. (ed.) Plant Hormones, vol. 72, pp. 457–478 (2005)
3. Wyatt, T.D.: Pheromones and signature mixtures: defining species-wide signals and variable cues for identity in both invertebrates and vertebrates. J. Comp. Physiol. A Neuroethol. Sens. Neural Behav. Physiol. **196**(10), 685–700 (2010). https://doi.org/10.1007/s00359-010-0564-y
4. Dube, F.F., Tadesse, K., Birgersson, G., Seyoum, E., Tekie, H., Ignell, R., Hill, S.R.: Fresh, dried or smoked? Repellent properties

of volatiles emitted from ethnomedicinal plant leaves against malaria and yellow fever vectors in Ethiopia. Malar. J. (2011). https://doi.org/10.1186/1475-2875-10-375
5. El-Sayed, A.M., Suckling, D.M., Wearing, C.H., Byers, J.A.: Potential of mass trapping for long-term pest management and eradication of invasive species. J. Econ. Entomol. **99**(5), 1550–1564 (2006)
6. Cook, S.M., Khan, Z.R., Pickett, J.A.: The use of push-pull strategies in integrated pest management. Annu. Rev. Entomol. **52**, 375–400 (2007). https://doi.org/10.1146/annurev.ento.52.110405.091407
7. Roelofs, W.L., Carde, R.T.: Responses of lepidoptera to synthetic sex-pheromone chemicals and their analogs. Annu. Rev. Entomol. **22**, 377–405 (1977). https://doi.org/10.1146/annurev.en.22.010177.002113
8. Pankiw, T., Page, R.E.: Brood pheromone modulates honeybee (*Apis mellifera* L.,) sucrose response thresholds. Behav. Ecol. Sociobiol. **49**(2–3), 206–213 (2001). https://doi.org/10.1007/s002650000282
9. Witzgall, P., Kirsch, P., Cork, A.: Sex pheromones and their impact on pest management. J. Chem. Ecol. **36**(1), 80–100 (2010). https://doi.org/10.1007/s10886-009-9737-y
10. Santos, I.P., Ramos, C., Ramos, J.L.G., Oliveira, R.F., Cunha, I.C.N.: Efficient association between pgf2 alpha and methyl 4-hydroxybenzoate sex pheromone prior to electroejaculation in dogs. Reprod. Domest. Anim. **48**(1), 160–164 (2013). https://doi.org/10.1111/j.1439-0531.2012.02123.x
11. Kutzler, M.A.: Semen collection in the dog. Theriogenology **64**(3), 747–754 (2005). https://doi.org/10.1016/j.theriogenology.2005.05.023
12. Siljander, E., Gries, R., Khaskin, G., Gries, G.: Identification of the airborne aggregation pheromone of the common bed bug, *Cimex lectularius*. J. Chem. Ecol. **34**(6), 708–718 (2008). https://doi.org/10.1007/s10886-008-9446-y
13. Suckling, D.M., Peck, R.W., Stringer, L.D., Snook, K., Banko, P.C.: Trail pheromone disruption of Argentine ant trail formation and foraging. J. Chem. Ecol. **36**(1), 122–128 (2010). https://doi.org/10.1007/s10886-009-9734-1
14. Suckling, D.M., Stringer, L.D., Bunn, B., El-Sayed, A.M., Vander Meer, R.K.: Trail pheromone disruption of red imported fire ant. J. Chem. Ecol. **36**(7), 744–750 (2010). https://doi.org/10.1007/s10886-010-9810-6
15. Tanaka, Y., Nishisue, K., Sunamura, E., Suzuki, S., Sakamoto, H., Fukumoto, T., Terayama, M., Tatsuki, S.: Trail-following disruption in the invasive Argentine ant with a synthetic trail pheromone component (Z)-9-hexadecenal. Sociobiology **54**(1), 139–152 (2009)
16. Wehrenfennig, C., Schott, M., Gasch, T., During, R., Vilcinskas, A., Kohl, C.D.: On-site airborne pheromone sensing. Anal. Bioanal. Chem. **405**(20), 6389–6403 (2013). https://doi.org/10.1007/s00216-013-7113-9
17. Dematteo, K.E., Rinas, M.A., Sede, M.M., Davenport, B., Arguelles, C.F., Lovett, K., Parker, P.G.: Detection dogs: an effective technique for bush dog surveys. J. Wildl. Manag. **73**(8), 1436–1440 (2009). https://doi.org/10.2193/2008-545
18. Kanzaki, R., Ando, N., Sakurai, T., Kazawa, T.: Understanding and reconstruction of the mobiligence of insects employing multiscale biological approaches and robotics. Adv. Robot. **22**(15), 1605–1628 (2008). https://doi.org/10.1163/156855308x368949
19. Schutz, S., Weissbecker, B., Koch, U.T., Hummel, H.E.: Detection of volatiles released by diseased potato tubers using a biosensor on the basis of intact insect antennae. Biosens. Bioelectron. **14**(2), 221–228 (1999). https://doi.org/10.1016/s0956-5663(98)00092-x
20. Schott, M., Wehrenfennig, C., Gasch, T., Vilcinskas, A.: Insect antenna-based biosensors for in situ detection of volatiles. In: Vilcinskas, A. (ed.) Yellow Biotechnology II: Insect Biotechnology in Plant Protection and Industry, vol. 136, pp. 101–122. Springer, Heidelberg (2013)
21. Tuccori, E., Persaud, K.C.: Pheromone detection using odorant binding protein sensors. In: 18th International Symposium on Olfaction and Electronic Nose (ISOEN). Fukuoka, Japan, pp. 25–27 (2019).
22. Riviere, S., Lartigue, A., Quennedey, B., Campanacci, V., Farine, J.P., Tegoni, M., Cambillau, C., Brossut, R.: A pheromone-binding protein from the cockroach *Leucophaea maderae*: cloning, expression and pheromone binding. Biochem. J. **371**, 573–579 (2003)
23. Katti, S., Lokhande, N., Gonzalez, D., Cassill, A., Renthal, R.: Quantitative analysis of pheromone-binding protein specificity. Insect Mol. Biol. **22**(1), 31–40 (2013). https://doi.org/10.1111/j.1365-2583.2012.01167.x
24. Wehrenfennig, C., Schott, M., Gasch, T., Meixner, D., During, R.A., Vilcinskas, A., Kohl, C.D.: An approach to sense pheromone concentration by pre-concentration and gas sensors. Phys. Status Solidi A Appl. Mater. Sci. **210**(5), 932–937 (2013). https://doi.org/10.1002/pssa.201200784
25. Moitra, P., Bhagat, D., Pratap, R., Bhattacharya, S.: A novel bioengineering approach to generate an eminent surface-functionalized template for selective detection of female sex pheromone of *Helicoverpa armigera*. Sci. Rep. (2016). https://doi.org/10.1038/srep37355
26. Suzuki, T., Nakakita, H., Kuwahara, Y.: Aggregation pheromone of *Tribolium freemani* HINTON (Coleoptera: Tenebrionidae). 1. Identification of the aggregation pheromone. Appl. Entomol. Zool. **22**(3), 340–347 (1987). https://doi.org/10.1303/aez.22.340
27. Suzuki, T.: 4,8-dimethyldecanal: the aggregation pheromone of the flour beetles, *Tribolium castaneum* and *T. confusum* (Coleoptera: Tenebrionidae). Agric. Biol. Chem. **44**(10), 2519–2520 (1980). https://doi.org/10.1080/00021369.1980.10864359
28. Hussain, A., Phillips, T.W., Mayhew, T.J., Aliniazee, M.T.: Pheromone biology and factors affecting its production in *Tribolium castaneum*. In: 6th International Working Conference on Stored-product Protection. Canberra, Australia, pp. 533–536 (1994)
29. Henzell, R.F., Lowe, M.D.: Sex attractant of the grass grub beetle. Science **168**(3934), 1005 (1970). https://doi.org/10.1126/science.168.3934.1005
30. Schoni, R., Hess, E., Blum, W., Ramstein, K.: The aggregation-attachment pheromone of the tropical bont tick *Amblyomma variegatum* Fabricius (Acari, Ixodidae): isolation, identification and action of its components. J. Insect Physiol. **30**(8), 613–618 (1984). https://doi.org/10.1016/0022-1910(84)90045-3
31. Cammaerts, M.C., Evershed, R.P., Morgan, E.D.: Comparative study of the mandibular gland secretion of four species of *Myrmica* ants. J. Insect Physiol. **27**(4), 225 (1981). https://doi.org/10.1016/0022-1910(81)90055-x
32. Ortius-Lechner, D., Maile, R., Morgan, E.D., Boomsma, J.J.: Metapleural gland secretion of the leaf-cutter ant *Acromyrmex octospinosus*: new compounds and their functional significance. J. Chem. Ecol. **26**(7), 1667–1683 (2000)
33. Yasui, H., Wakamura, S., Tanaka, S., Harano, K., Mochizuki, F., Nagayama, A., Hokama, Y., Arakaki, N.: Quantification of 2-butanol as a sex attractant pheromone and related alcohols emitted by individual white grub beetle, *Dasylepida ishigakiensis* (Coleoptera: Scarabaeidae). Appl. Entomol. Zool. **45**(1), 129–135 (2010). https://doi.org/10.1303/aez.2010.129
34. Ammagarahalli, B., Gemeno, C.: Interference of plant volatiles on pheromone receptor neurons of male *Grapholita molesta* (Lepidoptera: Tortricidae). J. Insect Physiol. **81**, 118–128 (2015). https://doi.org/10.1016/j.jinsphys.2015.07.009
35. McFarlane, J.E., Steeves, E., Alli, I.: Aggregation of larvae of the house cricket, *Acheta domesticus* (L.), by propionic acid present

in the excreta. J. Chem. Ecol. **9**(9), 1307 (1983). https://doi.org/10.1007/bf00994799
36. Mazomenos, B.E., Haniotakis, G.E.: Male olive fruit fly attraction to synthetic sex pheromone components in laboratory and field tests. J. Chem. Ecol. **11**(3), 397–405 (1985). https://doi.org/10.1007/bf01411425
37. Wood, D.L.: The role of pheromones, kairomones, and allomones in the host selection and colonization behavior of bark beetles. Annu. Rev. Entomol. **27**, 411–446 (1982). https://doi.org/10.1146/annurev.en.27.010182.002211
38. Wang, G.J., Fang, Y.N., Kim, P., Hayek, A., Weatherspoon, M.R., Perry, J.W., Sandhage, K.H., Marder, S.R., Jones, S.C.: Layer-by-layer dendritic growth of hyperbranched thin films for surface sol–gel syntheses of conformal, functional, nanocrystalline oxide coatings on complex 3d (bio)silica templates. Adv. Funct. Mater. **19**(17), 2768–2776 (2009). https://doi.org/10.1002/adfm.200900402
39. Davis, S.C., Sheppard, V.C., Begum, G., Cai, Y., Fang, Y.N., Berrigan, J.D., Kroger, N., Sandhage, K.H.: Rapid flow-through biocatalysis with high surface area, enzyme-loaded carbon and gold-bearing diatom frustule replicas. Adv. Funct. Mater. **23**(36), 4611–4620 (2013). https://doi.org/10.1002/adfm.201203758
40. Patel, S.V., Benz, M.: High-flux chemical sensors. US20120270205A1 (2012)
41. Lonergan, M.C., Severin, E.J., Doleman, B.J., Beaber, S.A., Grubb, R.H., Lewis, N.S.: Array-based vapor sensing using chemically sensitive, carbon black-polymer resistors. Chem. Mater. **8**(9), 2298–2312 (1996). https://doi.org/10.1021/cm960036j
42. Fang, Y.N., Hester, J.G.D., deGlee, B., Tuan, C.C., Brooke, P.D., Le, T.R., Wong, C.P., Tentzeris, M.M., Sandhage, K.H.: A novel, facile, layer-by-layer substrate surface modification for the fabrication of all-inkjet-printed flexible electronic devices on Kapton. J. Mater. Chem. C. **4**(29), 7052–7060 (2016). https://doi.org/10.1039/c6tc01066k
43. Fang, Y.N., Hester, J.G.D., Su, W.J., Chow, J.H., Sitaraman, S.K., Tentzeris, M.M.: A bio-enabled maximally mild layer-by-layer Kapton surface modification approach for the fabrication of all-inkjet-printed flexible electronic devices. Sci. Rep. (2016). https://doi.org/10.1038/srep39909
44. Fang, Y.N., Akbari, M., Sydanheimo, L., Ukkonen, L., Tentzeris, M.M.: Sensitivity enhancement of flexible gas sensors via conversion of inkjet-printed silver electrodes into porous gold counterparts. Sci. Rep. (2017). https://doi.org/10.1038/s41598-017-09174-5